Dean&Francis
ISSN 2959-6157

# Different Aerodynamic Performance of Gliders with Different Wing Shapes Referenced from Birds

**Wenwei Qiu**[1, *]

[1]Shenzhen Foreign Languages School (Group), Shenzhen, China
*Corresponding author: qiuwilliam27@gmail.com

**Abstract:**

A glider is a kind of aircraft that does not have power to drive. All its movement are controlled by air. Therefore, a high aerodynamic shape is required by a glider. Gliders nowadays have wings with significantly high aspect ratio. Its wing shape can be approximately seem as a rectangle or trapezoid. However, gliding is not a invention of human, there is a substantial number of animal is using this fly style, especially birds. Their wing shapes are more various, this might be due to the biological structure of birds, or it could be an inevitable result of natural selection. The objective of this paper is to compare and study the aerodynamic performance of wing shapes of two major gliding birds with the standard rectangular wing. The shape of the wing is inspired by seabirds and eagles. The experiment requires four models, Each model was thrown and its flight trajectory was recorded. The experimental results show that under the same aspect ratio, the wings of eagles exhibit higher aerodynamic performance. Its gliding Angle is significantly reduced, which means a higher lift-to-drag ratio. The possible reason for this is that the feathers on the outer side of the wing, On the higher aspect ratio, the shape of the wing only has a slight impact, with a decrease in the glide angle and a increase in speed. Nevertheless, The wing design that imitates the polyhedral wing of albatrosses has significantly improved flight efficiency. the meaning of this research lies in designing and optimizing the aerodynamic shape of the wing by referring to birds in nature, thereby enhancing the aerodynamic performance of the glider, which can made contributions in all fields of aerospace.

**Keywords:** Glider; Gliding angle; Lift-to-drag ratio; Aspect ratio; Albatross.

ISSN 2959-6157

# 1. Introduction

How could the ancients imagine that the kite in the sky would one day become a manned aircraft, and how could they have foreseen that one day humans would be able to fly like birds? The glider is the testament of human ingenuity. Its unique charm has become an indispensable part of the history of human aviation. The glider is not flying, it is gracefully falling[1]. As a member of aircraft, gliders do not have any power. It is so slender and light that it looks like a leaf floating in the air, and swayed freely in the gentle breeze. The truth is that the power and maneuverability of gliders both rely on air. In order to maintain long-time and long-distance flights without power, gliders require an exaggeratedly large lift-to-drag ratio and high flight stability, which demands extreme aerodynamic design. In this sense, the glider can be regarded as the condensation and application of human mastery of aerodynamics technology. However, it is undeniable that birds are also excellent fliers. If humans were to imitate the flight techniques and methods of birds, could this lead to further improvements in the flight efficiency of aircraft?

Nowadays, research on glider wings often focuses on the size of their aspect ratio and the selection of airfoil. Experiments show that a higher aspect ratio of the wing can significantly increase the lift-to-drag ratio [2]. This can also be easily found in nature. Wandering albatrosses with high span-chord ratios have one of the strongest gliding ability and highest flight efficiency among extent birds[3]. The selection of airfoils for gliders is diverse, with the prerequisite of having a high lift coefficient and a low drag coefficient. Natural laminar flow airfoils (NLF) are a common choice for gliders. This type of airfoil can delay the generation of turbulence, hence the drag can be significantly reduced while maintaining the lift force unchanged, which can enhance the aerodynamic performance of the glider and extend the gliding distance and the time staying in the air[4]. Additionally, Aircraft that require a high lift-to-drag ratio, such as gliders typically use trapezoidal wings or the combination of rectangles and trapezoids, which means that the chord length at the wingtip is shorter than that at the wing root. The wind tunnel experiments conducted by NASA have verified that trapezoidal wing have advantages in reducing induced drag and increasing lift coefficient [5]. In recent years, a significant progress has been made in the research on the flight mechanisms of birds and the shapes of their wings, especially the wings of seabirds and raptors. The research of seabirds mainly focused on the dynamic gliding of albatross and its morphing wing. The research on raptors not only have strong gliding ability, but also a large carrying capacity focuses on its morphing wing and the wingtip slots.

The shapes of bird wings is the result of natural selection over million of years. they have undergone a substantial number of iterations and optimizations over a long period of time. These can provide ideas and directions for our design. Therefore, the objective of the paper is to optimize and explore new glider wing shapes by referring the shapes of bird wings, in order to enhance the flight efficiency of the glider. To achieve the goal, four models were created. Two of them are basic rectangular wings with different aspect ratios, and the other two are based on the wings of the albatrosses and eagles. Four models were thrown and their flight trajectories were recorded. From the flight trajectory, the flight speed and the gliding angle can be obtained, thereby inferring the flight efficiency. Finally, these data were compared and analyzed.

# 2. Methodology

## 2.1 Experimental Tool

The flight trajectory of the models was recorded by camera, and the videos were uploaded to the Tracher, a motion analysis software. The icon and interface of Tracher will be illustrate in Figure 1 and Figure 2 respectively below. The coordinates of the model's head in each frame in the videos were manually marked. Therefore, only the position parameters of the models at each time can be obtained from the video. Its flight speed and gliding angle can only be obtained by calculation.

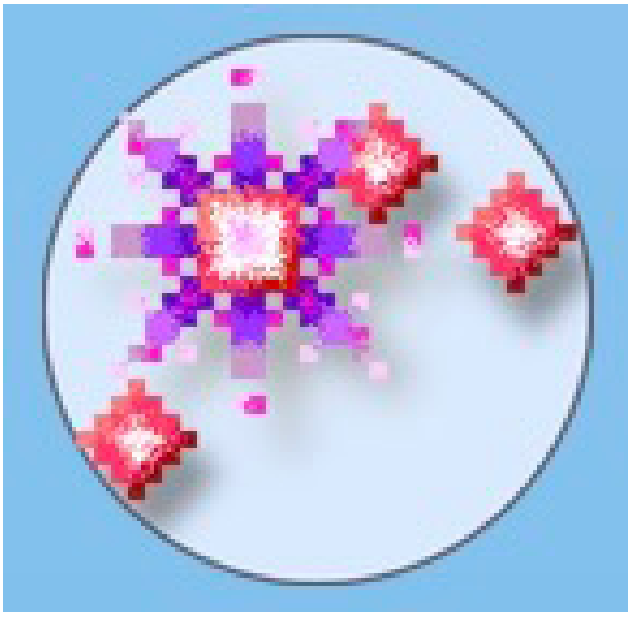

**Fig. 1 Tracher Icon**

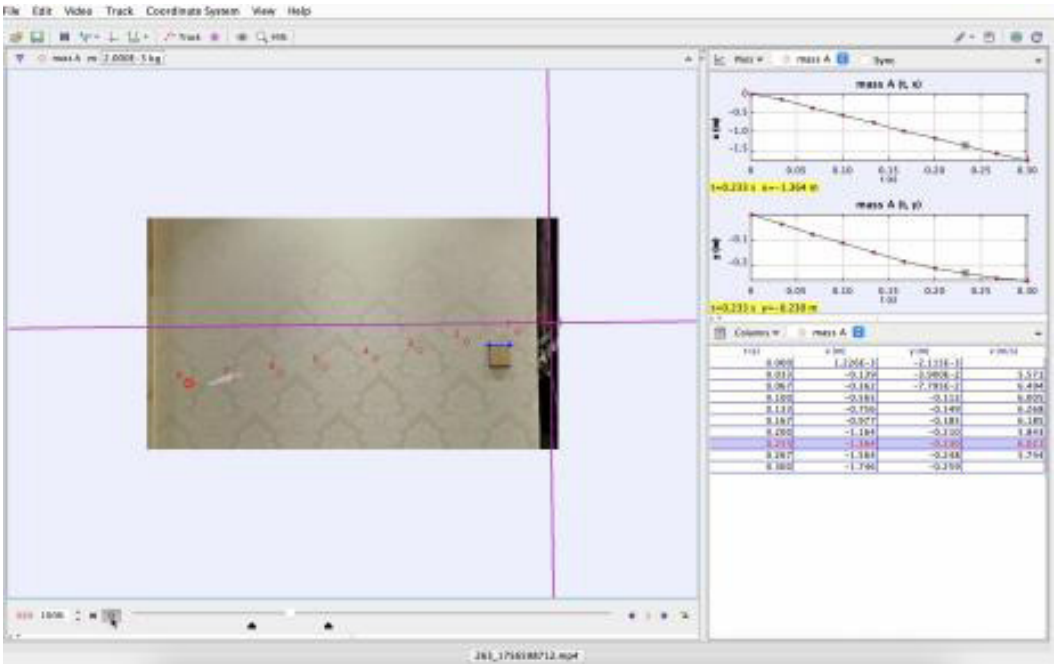

**Fig. 2 Interface of Tracher**

## 2.2 Mathematical Formulations and Theoretical Background

During the experiment, the wing chord was regarded as parallel to the relative airflow direction, which means the angle of attack(AoA) is zero. So the lift-to-drag ratio(L/D) of the aircraft can be calculated based on its glide Angle(θ). Meanwhile, the gliding velocity of each model is also regarded as a constant, which implies that the horizontal and vertical resultant force acting on the model is zero. For the specific free-body diagram, please refer to Figure 3.

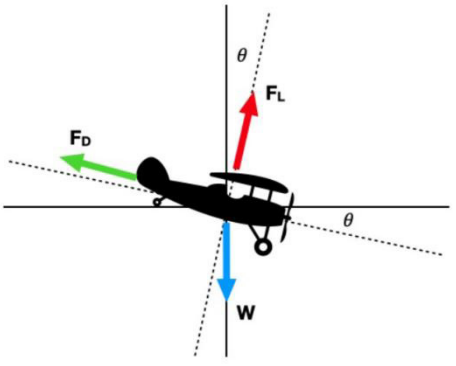


**Fig 3. Free-Body Diagram of Aircraft**

Projecting drag(FD) and lift(FL) onto the horizontal directions, we have:

$$F_D cos\theta = F_L sin\theta \tag{1}$$

From the horizontal equation, we have:

$$\frac{F_L}{F_D} = \frac{1}{tan\theta} \tag{2}$$

Therefore, the lift-to-drag ratio of the model is the reciprocal of its glide angle.

In addition, the relationship formula between wing area(S), wingspan(b) and mean aerodynamic chord(c) length will be illustrate as follow:

$$S = b \times c \tag{3}$$

Since the shape of the wing in the experimental model is irregular, the average aerodynamic chord length is calculated based on the wing area and the wing span:

$$c = \frac{S}{b} \tag{4}$$

Therefore, aspect ratio(λ) can be calculated:

$$\lambda = \frac{b}{c} = \frac{b^2}{S} \tag{5}$$

The formula for the speed(vn) about the horizontal coordinate(xn) and vertical coordinate(yn) of the model at a certain time(Tn) will be presented below:

$$v_n = \frac{\sqrt{\left(x_{n-1} - x_n\right)^2 + \left(y_{n-1} - y_n\right)^2}}{T_n - T_{n-1}} \tag{6}$$

The formula for the gliding angle(θ) about the horizontal coordinate(xn) and vertical coordinate(yn) of the model at a certain time(Tn) will be presented below:

$$\theta = tan^{-1}\frac{y_{n-1} - y_n}{x_{n-1} - x_n} \tag{7}$$

Therefore, the lift-to-drag ratio(E) at certain time can be

ISSN 2959-6157

expressed by the following formula:

$$E = \frac{x_{n-1} - x_n}{y_{n-1} - y_n} \quad (8)$$

# 3. Model Design

## 3.1 Common Parameters

The focus of this study is the influence of wing shape on gliding efficiency, therefore the only variable that the model will change is the shape of the wing, and the area of the wings and the weight of the model must be constant. In this experiment, the wing area of each model is 4200 $mm^2$ , and the weight of each model is 2g .

Totally four models were made, and each model has different wing shapes, they are model 1, model 2, model 3, and model 4 respectively. To control for variables, all four models have the same "V" shape empennage. The Figure 4 below shows four physical models.

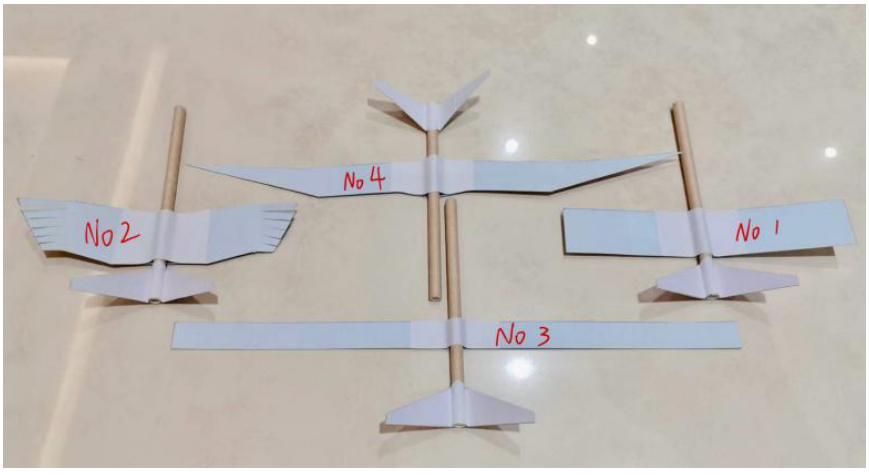


**Fig 4. Picture of Four Models**

The basic parameters of the model are presented in the following Table 1:

**Table 1. Model Parameter**

| Model | Area(cm^3) | Span(cm) | Mean Chord Length(cm) | Aspect Ratio | Anhedral Angle(degree) |
|---|---|---|---|---|---|
| Model 1 | 42.0 | 15.0 | 2.80 | 5.36 | 0 |
| Model 2 | | | | | |
| Model 3 | | 29.0 | 1.45 | 20.0 | |
| Model 4 | | | | | |
| Model 4(new) | | | | | 20 |

3.2 the Parameters of each One

Two of them is simple rectangular wing with different span-chord ratio. The designs of the other two models are based on two types of birds in nature that possess extremely strong gliding abilities. they are the bird from accipitriformes order and procellariiformes order. The aspect ratio of the wings of birds belonging to the accipitriformes is smaller compared to that of birds belonging to the procellariiformes. The details of the four models will be demonstrated separately below:

### 3.2.1 Model 1

The wing shape of this model is rectangular, and it was designed to have a relatively smaller aspect ratio. Because it is the control model of the raptor wing shape. The span, average aerodynamic chord length, and aspect ratio of the model 1 is 150mm , 28mm , and 5.36 respectively. Figure 5 shows Wing Planform Layout for model 1.

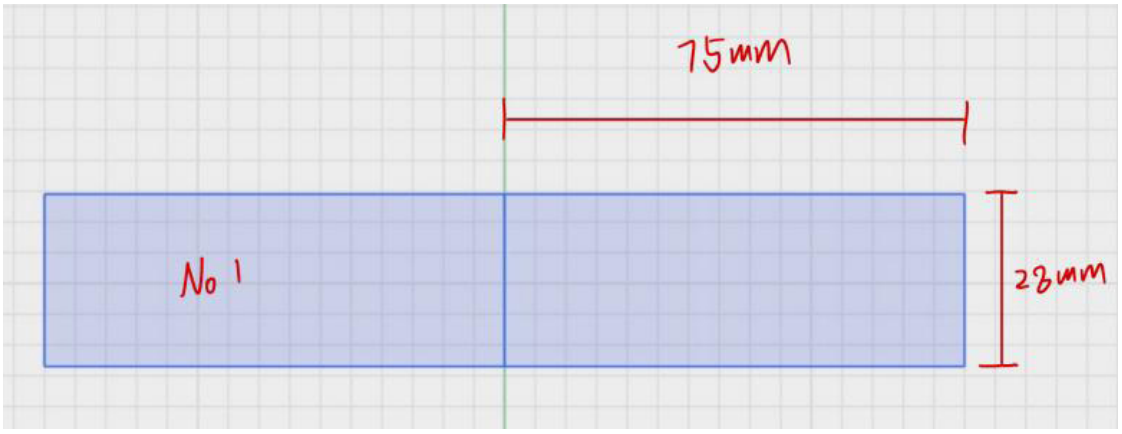


**Fig 5. Wing Planform Layout for Model 1**

### 3.2.2 Model 2

The wing design of this model is based on that of the raptor. The raptor can adjust its shape of wings based on its flight and condition[6]. Since the research subject is the gliders, the paper will choose the wing configuration of fully extended at low speeds. The wing of most of raptor is slotted high-lift wing with wingtip feathers[7]. Wingtip slots is regarded as a feature that helps enhance the soaring performance[8]. For the the wing shape of a raptor, please refer to figure 6.

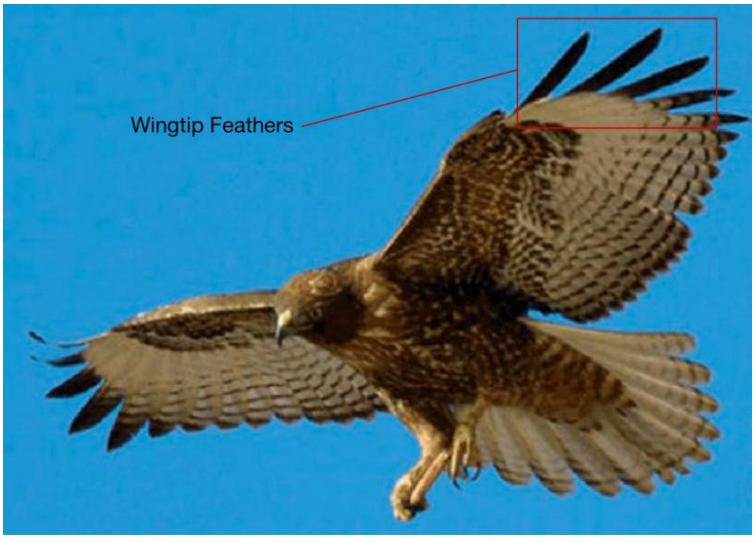


**Fig 6. Red Tailed Hawk[7]**

The span, average aerodynamic chord length, and aspect ratio of the model 2 is 150mm , 28mm , and 5.36 respectively. Figure 7 shows Wing Planform Layout for model 2.

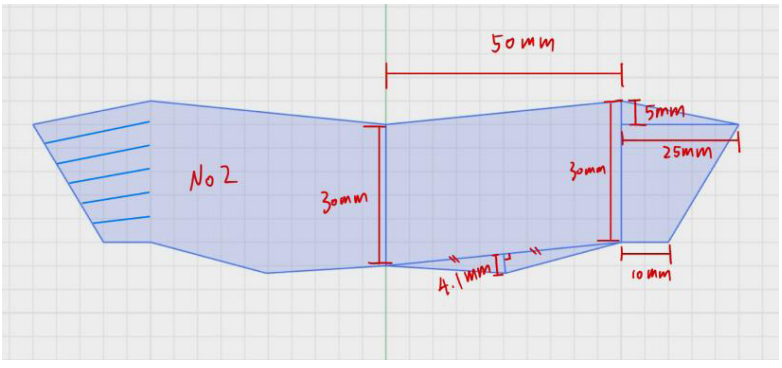


**Fig 7. Wing Planform Layout for Model 2**

ISSN 2959-6157

### 3.2.3 Model 3

The wing shape of this model is rectangular, and it was designed to have a relatively larger aspect ratio. Because it is the control model of the albatrosses wing shape. The span, average aerodynamic chord length, and aspect ratio of the model 3 is 290mm , 14.5mm , and 20 respectively. Figure 8 shows Wing Planform Layout for model 3.


**Fig 8. Wing Planform Layout for Model 3**

### 3.2.4 Model 4

The wing design of this model is based on that of the albatrosses. This is a kind of gliding high aspect ratio pointed wing[7]. For the the wing shape of an albatross, please refer to figure 9.

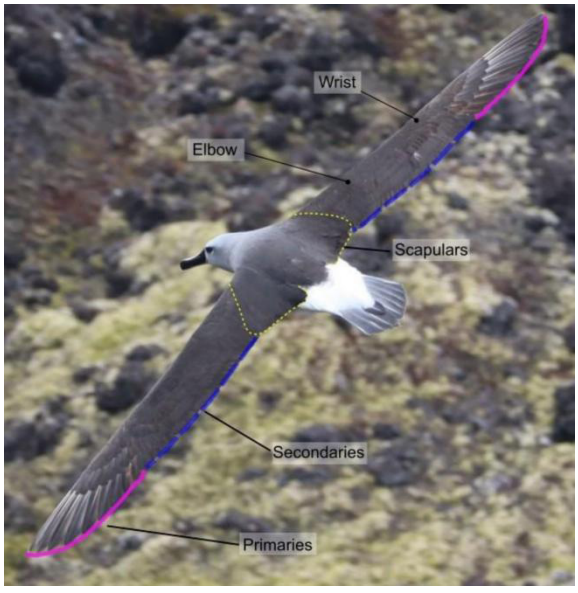


**Fig 9. Grey-Headed Albatross[9]**

The span, average aerodynamic chord length, and aspect ratio of the model 4 is 290mm, 14.5mm, and 20 respectively. Figure 10 shows Wing Planform Layout for model 4.

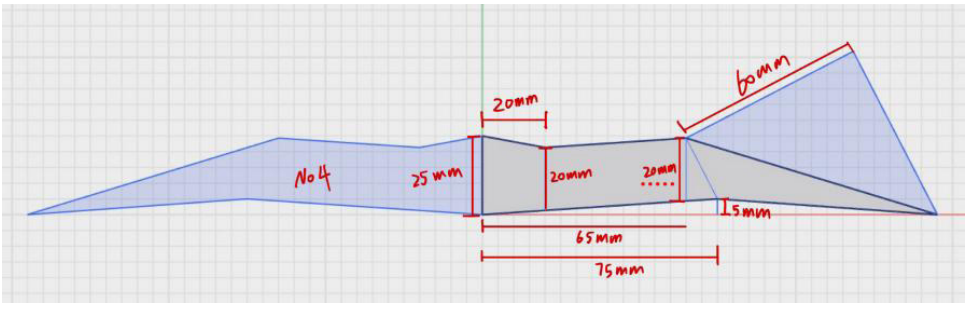


**Fig 10. Wing Planform Layout for Model 4**

### 3.2.5 Model 4(new)

During the period of leeward descent, which is closer to the flight conditions of gliders, albatross will bend the wingtips downward. the wingtip of the albatross will be anhedral like Figure 11 [10].

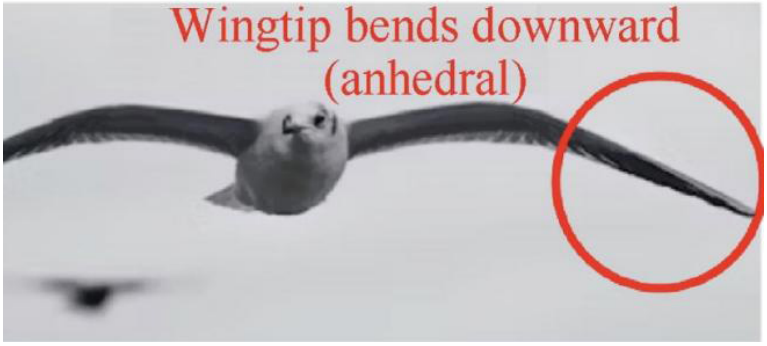


**Fig 11. Albatross Wing Morphing during the Period of Leeward Descent[10]**

Therefore, after all the data of model 4 had been measured, the wings of model 4 was folded down approximately 20 degrees at the middle section. The processed model 4 is referred to model 4(new).

# 4. Result

## 4.1 Experimental Data

The experimental data will be presented in the following table 2.

**Table 2. Experimental Data**

| Model 1 | | | | | |
|---|---|---|---|---|---|
| t(On Video) | t(s) | x(m) | y(m) | v(m/s) | θ(Radian) |
| 0.03 | 0.00 | 0.00 | 0.00 | - | 0.36 |
| 0.07 | 0.03 | -0.21 | -0.08 | 6.28 | 0.30 |
| 0.10 | 0.07 | -0.40 | -0.14 | 6.00 | 0.27 |
| 0.13 | 0.10 | -0.59 | -0.19 | 6.01 | 0.23 |
| 0.17 | 0.13 | -0.78 | -0.24 | 5.86 | 0.20 |
| 0.20 | 0.17 | -0.97 | -0.28 | 5.48 | 0.17 |
| 0.23 | 0.20 | -1.14 | -0.31 | 5.36 | 0.15 |
| 0.27 | 0.23 | -1.32 | -0.33 | 5.27 | 0.16 |
| 0.30 | 0.27 | -1.49 | -0.36 | 5.27 | 0.16 |
| 0.33 | 0.30 | -1.67 | -0.39 | Average: 5.72 | Average: 0.22 |
| Model 2 | | | | | |
| t(On Video) | t(s) | x(m) | y(m) | v(m/s) | θ(Radian) |
| 0.07 | 0.00 | 0.00 | 0.00 | - | 0.17 |
| 0.10 | 0.03 | -0.19 | -0.03 | 5.98 | 0.16 |
| 0.13 | 0.07 | -0.39 | -0.07 | 5.68 | 0.12 |
| 0.17 | 0.10 | -0.57 | -0.09 | 5.61 | 0.09 |
| 0.20 | 0.13 | -0.76 | -0.11 | 5.62 | 0.07 |
| 0.23 | 0.17 | -0.94 | -0.12 | 5.29 | 0.05 |
| 0.27 | 0.20 | -1.12 | -0.13 | 5.25 | 0.03 |
| 0.30 | 0.23 | -1.29 | -0.13 | 5.87 | 0.03 |
| 0.33 | 0.27 | -1.51 | -0.14 | 5.97 | 0.07 |
| 0.37 | 0.30 | -1.69 | -0.15 | Average: 5.65 | Average: 0.09 |
| Model 3 | | | | | |
| t(On Video) | t(s) | x(m) | y(m) | v(m/s) | θ(Radian) |
| 0.00 | 0.00 | 0.00 | 0.00 | - | 0.26 |

ISSN 2959-6157

| | | | | | |
|---|---|---|---|---|---|
| 0.03 | 0.03 | -0.14 | -0.04 | 5.57 | 0.17 |
| 0.07 | 0.07 | -0.36 | -0.08 | 6.49 | 0.17 |
| 0.10 | 0.10 | -0.57 | -0.11 | 6.01 | 0.19 |
| 0.13 | 0.13 | -0.76 | -0.15 | 6.27 | 0.16 |
| 0.17 | 0.17 | -0.98 | -0.19 | 6.19 | 0.13 |
| 0.20 | 0.20 | -1.16 | -0.21 | 5.84 | 0.10 |
| 0.23 | 0.23 | -1.36 | -0.23 | 6.02 | 0.09 |
| 0.27 | 0.27 | -1.56 | -0.25 | 5.74 | 0.06 |
| 0.30 | 0.30 | -1.75 | -0.26 | Average: 5.82 | Average: 0.148 |
| Model 4 | | | | | |
| t(On Video) | t(s) | x(m) | y(m) | v(m/s) | θ(Radian) |
| 0.00 | 0.00 | 0.00 | 0.00 | - | 0.16 |
| 0.03 | 0.03 | -0.20 | -0.03 | 6.08 | 0.16 |
| 0.07 | 0.07 | -0.42 | -0.07 | 6.67 | 0.17 |
| 0.10 | 0.10 | -0.62 | -0.10 | 6.09 | 0.16 |
| 0.13 | 0.13 | -0.80 | -0.13 | 5.56 | 0.16 |
| 0.17 | 0.17 | -1.00 | -0.16 | 5.81 | 0.13 |
| 0.20 | 0.20 | -1.21 | -0.19 | 6.54 | 0.13 |
| 0.23 | 0.23 | -1.41 | -0.22 | 6.02 | 0.13 |
| 0.27 | 0.27 | -1.60 | -0.24 | 5.79 | 0.14 |
| 0.30 | 0.30 | -1.80 | -0.27 | Average: 6.07 | Average: 0.149 |
| Model 4(new) | | | | | |
| t(On Video) | t(s) | x(m) | y(m) | v(m/s) | θ(Radian) |
| 0.03 | 0.00 | 0.00 | 0.00 | - | 0.10 |
| 0.07 | 0.04 | -0.22 | -0.02 | 5.96 | 0.10 |
| 0.10 | 0.07 | -0.40 | -0.04 | 5.66 | 0.05 |
| 0.13 | 0.10 | -0.59 | -0.05 | 5.40 | 0.02 |
| 0.17 | 0.14 | -0.76 | -0.05 | 4.83 | 0.01 |
| 0.20 | 0.17 | -0.91 | -0.05 | 4.62 | 0.03 |
| 0.23 | 0.20 | -1.06 | -0.06 | 4.07 | 0.05 |
| 0.27 | 0.24 | -1.19 | -0.06 | 3.62 | 0.04 |
| 0.30 | 0.27 | -1.30 | -0.07 | 3.88 | 0.02 |
| 0.33 | 0.30 | -1.44 | -0.07 | Average: 4.81 | Average: 0.04 |

### 4.2 Relationship Diagrams

From the table, we can obtain a series of relationship diagrams, including the diagrams showing the relationship between the time and the glide angle of the models, the diagrams showing the relationship between the time and the speed of the models, and the diagrams depicting the glide trajectories of the models. They will be shown in Figures 12, 13 and 14 respectively.

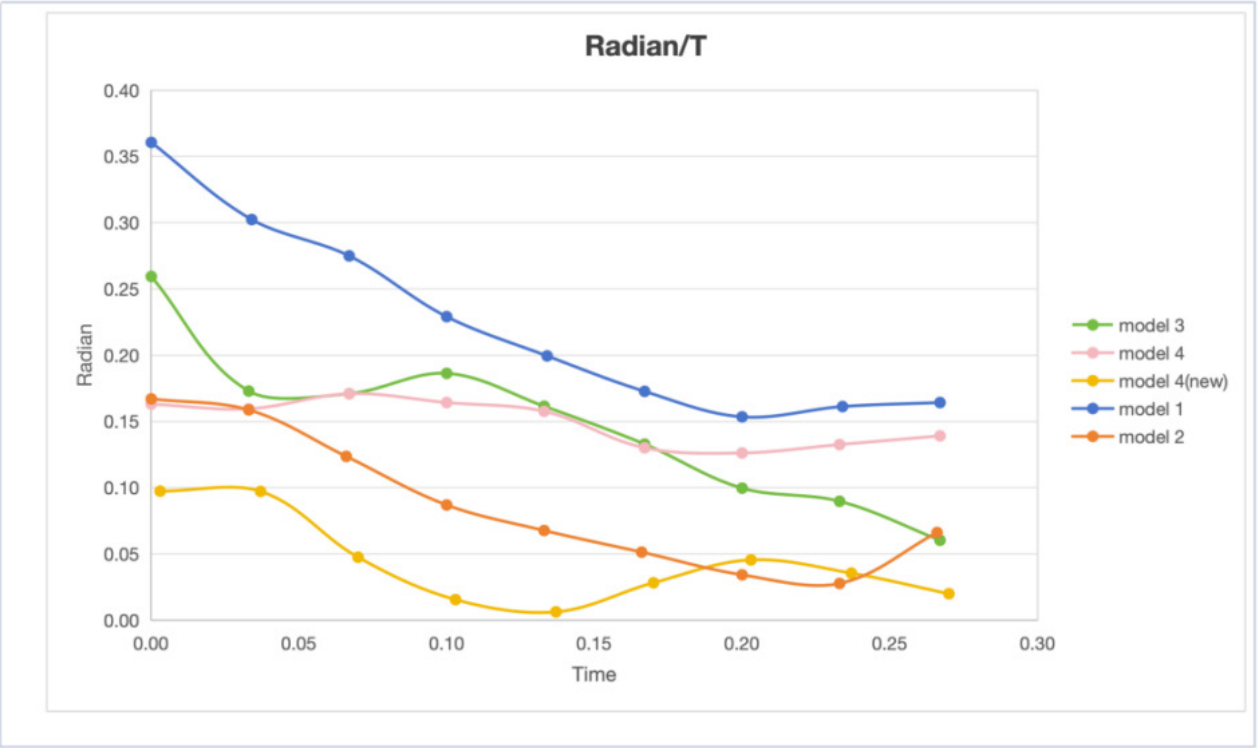


**Fig 12. Relationship between the Time and the Glide Angle of the Models**

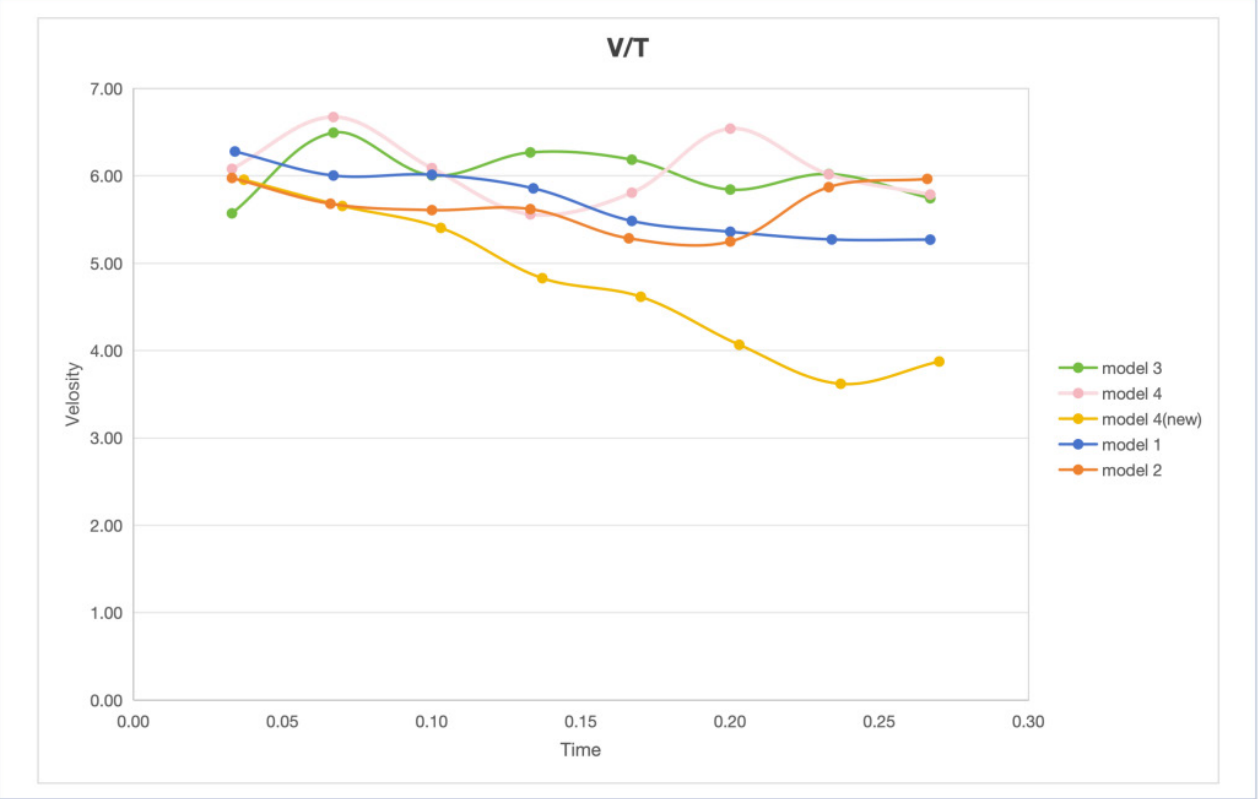


**Fig 13. Relationship between the Time and the Speed of the Models**

ISSN 2959-6157

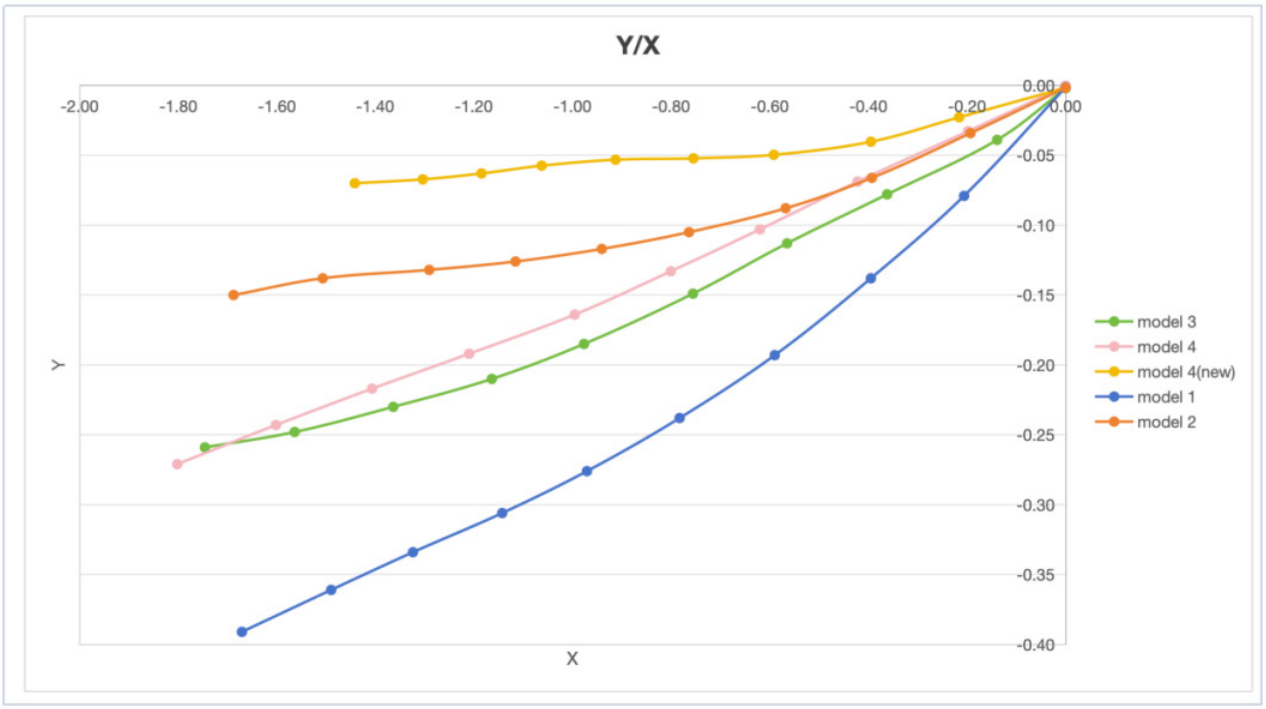


**Fig 14. glide trajectories of the models**

## 5. Discussion

### 5.1 Comparison and Discussion of Model 1 and Model 2

The following Figure 15 demonstrate the gliding trajectories of the two models:

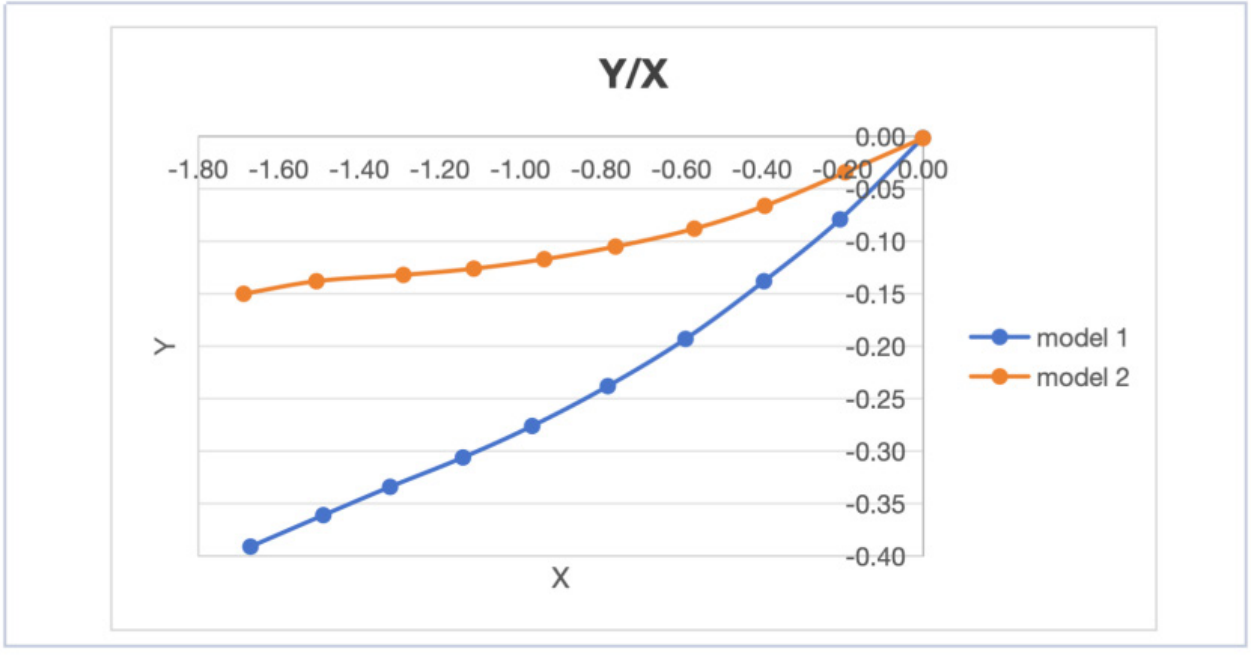


**Fig 15. The Trajectories of Model 1 and Model 2**

It can be obviously seen from the figure 15 that the glide angle of Model Two is significantly smaller than that of

model 1. This means that model 2 has a higher lift-to-drag ratio. The average sliding angle of model 1 is 0.22 radian, while that of model 2 is 0.09 radian. By calculation, the lift-to-drag ratio of the model 1 is 4.47, and that of model 2 is 11.08. This means that, with the same aspect ratio, the wings of raptors have a higher gliding efficiency. This is largely due to the slot design at the tip of the wing. The experiment shows that the airflow disturbance caused by the formation of slots between multiple wingtips can significantly increase the lift coefficient, which , to some extent, also explains the phenomenon of energy conservation during the flight of birds[11]. In addition, The gliding speed of two model are slightly different. The average flight speed of model 1 is 5.72 meters per second, while that of model 2 is 5.65 meters per second. There may be two reasons for the speed difference. Firstly, a lower rate of decline for model 2 will contribute to a slower conversion of gravitational potential energy into kinetic energy. Secondly, to some extent the slots on the wingtips will increase the drag force.

### 5.2 Comparison and Discussion of Model 3, Model 4 and Model 4(new)

The following Figure 16 demonstrate the gliding trajectories of the these three models:

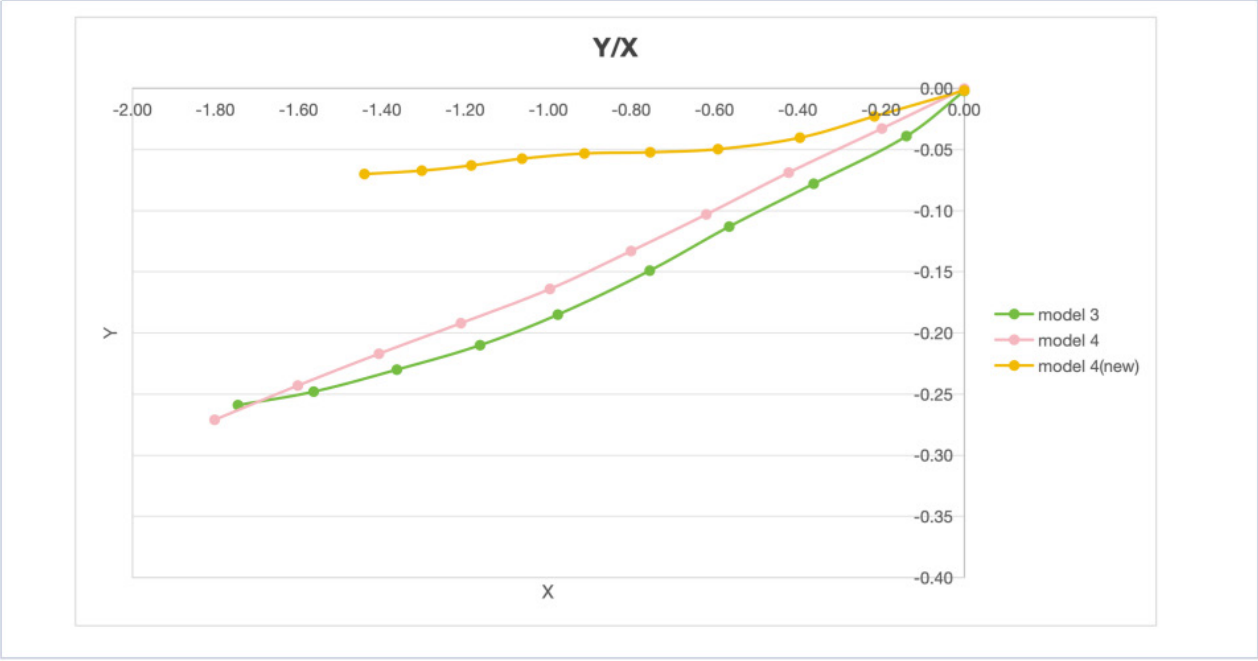


**Fig 16. The Trajectories of Model 3, Model 4 and Model 4(new)**

From the curves of model 3 and model 4, it can be seen that under the condition of a large aspect ratio, the wing shape has no significant impact on the gliding efficiency. Their gliding angles were very close. The average gliding angle of model 3 and model 4 are 0.148 radian and 0.149 radian respectively. By calculation, the lift-to-drag ratio of the model 1 is 6.71, and that of model 2 is 6.66. Such minor differences can not illustrate anything, because there are various uncontrollable factors in the experiment itself. The gliding speeds of the two models also differ little. The average flight speed of model 3 is 5.82 meters per second, while that of model 4 is 6.07 meters per second. The slightly faster speed of model 4 might be attributed to its lower drag coefficient compared to model 3. The special wing shape of model 4 causes the outer part of the wing can be regard as swept-back wing, and it has extremely sharp wingtips. Studies have shown that, to a certain extent, this shape can reduce induced drag[12]. From the curve of model 4(new), it can be seen that model 4(new) has the smallest average gliding angle that is 0.04 radian. This means that model 4(new) has the highest lift-to-drag ratio(25.00) compared to the other four models, which demonstrates its extremely high gliding efficiency. This downward-curving wing has a slightly higher lift coefficient than a straight wing when the angle of attack is between 2 and 4 degrees[10]. Meanwhile,this kind of morphing wing shows a decrease in downwash airflow intensity, thereby lowering the induced drag[10]. This might be the reason why model 4(new) has a relatively high lift coefficient. However, the average sliding speed of model 4(new) is only 5 meters per second, which is very slow. The main reason is that the extremely low descent rate

ISSN 2959-6157

results in a slow energy conversion between the gravitational potential energy and kinetic energy.

## 6. Limitations and future outlooks

This experiment was rather rudimentary. This results in the inability to perfectly control the variables, and there are many uncontrollable factors during the experiment. For instance, the initial speed of the models when they were thrown might different. In addition, The wings of the models are made of paper which are easily affected by air humidity. This will cause the model wings to undergo irregular deformations, such as twisting, bending and so on. Among them, the twisting of the wings and the deformation of the empennage have a relatively significant impact. Furthermore, in this experiment, each model underwent multiple projections. However, only one flight trajectory that best represents the model flight state was selected for analysis. Overall, the experimental data in this article is not accurate enough. The data only have the significance of analyzing trends and making comparisons.

The research in this paper is limited to the gliding efficiency of a fixed wing. Nevertheless, in nature, the flight of birds is dynamic flight, and their wings will change according to the flight state. Further research may need to focus on the mechanism of its deformation with a higher flight efficiency. This dynamic flight can fully utilize the energy of atmospheric movements. The future research direction might be deformable wings through some form of hinge or flexible wing structure. Achieving a high-efficiency dynamic flight similar to that of an albatross by using deformable wings will become the main target.

## 7. Conclusion

Believing that the outcome of natural selection and the imitation of the shape of bird wings are the central ideas of this paper. From the experimental results, it can be seen that at a smaller aspect ratio, the wings of the raptor have a relatively high gliding efficiency, which may be attributed to the design of the slots at the wingtips. In addition, Under conditions of high aspect ratio, merely referring to the wing shape of the albatross will not significantly improve the gliding efficiency. The secret to the albatross' extremely high gliding efficiency is its morphing wings. The downward-curving wings can significantly increase the lift coefficient and reduce the induced drag. The significance of this research is extensive. The main purpose is to optimize the aerodynamic shape of the glider, in order to improve the gliding efficiency of the glider. At the same time, it can also provide new ideas and directions for the manufacturing and design of aircraft.

## References

[1] Khatoon K. Design and Performance Evaluation of Polyhedral Swept Back Hing Wing Chuck Glider for Better L/D Ratio[J]. International Journal of Mechanical and Production Engineering Research and Development (IJMPERD), 2018, 8: 1-12.

[2] Zhang Fandong. The Relationship Between Aspect Ratio and Lift/Drag Ratio[J]. Highlights Sci. Eng. Technol, 2024, 81: 411-417.

[3] Schoombie S, Wilson R P, Ryan P G. Wind driven effects on the fine-scale flight behaviour of dynamic soaring wandering albatrosses[J]. Marine Ecology Progress Series, 2023.

[4] Streit T, Wedler S, Kruse M. DLR natural and hybrid transonic laminar wing design incorporating new methodologies[J]. The Aeronautical Journal, 2015, 119(1221): 1303-1326.

[5] Rumsey C L, Lee-Rausch E M. NASA trapezoidal wing computations including transition and advanced turbulence modeling[J]. Journal of Aircraft, 2015, 52(2): 496-509.

[6] Cheney J A, Stevenson J P J, Durston N E, et al. Raptor wing morphing with flight speed[J]. Journal of The Royal Society Interface, 2021, 18(180): 20210349.

[7] Liu Dan, Song Bifeng, Yang Wenqing, et al. A brief review on aerodynamic performance of wingtip slots and research prospect[J]. Journal of Bionic Engineering, 2021, 18(6): 1255-1279.

[8] KleinHeerenbrink M, Johansson L C, Hedenström A. Multi-cored vortices support function of slotted wing tips of birds in gliding and flapping flight[J]. Journal of the Royal Society Interface, 2017, 14(130): 20170099.

[9] Schoombie J. Investigating aerodynamic factors in wind-driven grey-headed albatross crash-landings[J]. 2024.

[10] Wang Wei, An Weigang, Song Bifeng. Effect of wing morphing on stability and energy harvesting in albatross dynamic soaring[J]. Chinese Journal of Aeronautics, 2024, 37(11): 317-334.

[11] Liu Dan, Song Bifeng, Yang Wenqing, et al. Unsteady characteristic research on aerodynamic interaction of slotted wingtip in flapping kinematics[J]. Chinese Journal of Aeronautics, 2022, 35(4): 82-101.

[12] Ayvazian A, Alcocel I C, Gowree E R. On bio-inspired induced drag reduction techniques[C]//56th 3AF International Conference on Applied Aerodynamics. 2022: 0.